Coordinate-Tracing Model of Light Forward Scattered by Turbid Media

Liu Wu(吴　柳)[1]　　Zhe Li(李　哲)[1]　　Jiasheng Wang(汪家升)[1]　　Xiangqun Xu(徐向群)[2]

([1] *Department of Physics，Beijing Jiaotong University，Beijing* 100044，*China*
[2] *School of Science，Zhejiang Sci-Tech University，Hangzhou，Zhejiang* 310018，*China*)

Abstract　Optical techniques based on measuring scattering properties of bio-tissues have a potential to determine internal physiological state. For tissue imaging，the least-scattered photons arriving at a detector may have a significant effect on the development of imaging algorithms. Tracing least-scattered photons may be helpful for further understanding of imaging mechanisms within current high-resolution optical-imaging techniques. Based on the vertex-propagator，a coordinate-tracing model is developed to search probabilities for least-scattered photons traversing in a scattering medium. Integral expressions for photon experiencing any time scattering events are obtained. Compared with the methods based on both geometrical tracing and Monte Carlo simulation，our model is simpler and easier for programming.

Key words　scattering；turbid media；imaging algorithm；biomedical optics
CLCN：O242.2；TN012　　　　**Document Code**：A　　　　**doi**：10.3788/CJL20093610.2510

1　Introduction

Understanding of the interaction of light within tissue at a cellular level will promote the development of optical diagnostic techniques. Optical techniques are potentially capable of rapid，non-invasive assessment of tissue pathology. In the past years，a number of techniques have been developed that rely in some manners on measuring the scattering properties of tissue to determine its physiological state. These techniques range from direct imaging methods such as confocal microscopy[1]，optical coherence tomography (OCT)[2]，and photoacoustic imaging[3]，to relatively indirect approaches including elastic-scattering spectroscopy[4] and photon migration[5].

OCT uses low coherence interferometry to produce a two-dimensional image of optical scattering from both internal tissue microstructures[6~8] and blood[9,10]. The main problem with light tomography of biological tissues，which are highly light-scattering media，is retrieving information about the properties and the structures of the tissue from the static and dynamic characteristics of outgoing light. To tackle the problem，it is necessary to assume a theoretical model of the scattering medium and formulate mathematically a light-propagation problem to be solved analytically or numerically. Obviously，Monte Carlo simulation techniques can be used to trace stochastically the light propagating in the medium[11]，but it is time consuming.

There are a few general theoretical approaches available for considering light propagation in scattering materials，e. g.，light-transport theory[12]，light-diffusion approximation[12~15]，multiflux radiative transfer theory[12,16~18]，probabilistic random-walk theory[19~21]，and photon path analysis[22,23]. For least-scattered photons that arrive at a detector through a turbid medium like tissue，Jacques *et al.* [24] introduced a path integral description to predict the early-arriving photons to the detector. Wang *et al.* [25] introduced a theory based on the vertex/propagator model to find the least-scattered photons probabilities by tracing photons geometrically. However，the geometrical expression of photon history is too complex to be obtained for more than double interactions. In this paper，a modified coordinate tracing model based on vertex-propagator is developed to find the probabilities for least-scattered photons traversing in a scattering medium，and integral forms of scattered photon probability are obtained for photon experiencing any time scattering events. The new model is very simple and easy for programming，therefore the tracing

processes are relatively timesaving. Moreover, our results are in very good agreement with Wang's work and Monte Carlo simulation.

2 Theory

2.1 Vertex/propagator description

Consider a photon scattered in a homogeneous scattering medium with specific scattering coefficient μ_s, extinction coefficient μ_t, and anisotropy parameter g. As illustrated in Fig. 1, for the ith scattering history, the displacement vectors of the photon before and after the ith scattered are $\boldsymbol{r}_{i-1}$ and $\boldsymbol{r}_i$, respectively, and the scattering angle θ_i is determined by

$$\boldsymbol{r}_{i-1} \cdot \boldsymbol{r}_i = r_{i-1} \cdot r_i \cos \theta_i. \quad (1)$$

So the probability density of the photon from the starting point O_{i-1} to the end point O_{i+1} after the ith scattering at point O_i can be written as

$$\Gamma_i = \exp(-\mu_t r_{i-1}) p(\cos \theta_i) \, \mu_s \exp(-\mu_t r_i), \quad (2)$$

where $\exp(-\mu_t r_{i-1})$ and $\exp(-\mu_t r_i)$ are the propagators before and after scattering at point O_i, respectively, $p(\cos \theta_i)\mu_s$ is the vertex term, and $p(\cos \theta_i)$ represents the phase function of the medium, which is often assumed to take a particular form firstly described by Henyey et al.[26]:

$$p(\cos \theta) = \frac{1 - g^2}{(1 + g^2 - 2g\cos \theta)^{3/2}}, \quad (3)$$

where g is the mean value of $\cos \theta$. In the case of isotropic scattering, $p(\cos \theta_i) = 1/(4\pi)$.

After N times scattered, the photon moves from the start point O to the end point E, the probability density corresponding to the displacement, $\boldsymbol{r} = \boldsymbol{r}_0 + \boldsymbol{r}_1 + \boldsymbol{r}_2 + \cdots + \boldsymbol{r}_N$, is

$$\Gamma(r) = \exp(-\mu_t r_0) p(\cos \theta_1) \times$$
$$\mu_s \exp(-\mu_t r_1) p(\cos \theta_2) \mu_s \exp(-\mu_t r_2) \cdots$$
$$\exp(-\mu_t r_{N-1}) \, p(\cos \theta_N) \mu_s \, \exp(-\mu_t r_N). \quad (4)$$

The reflection at the interface between the media must be taken into account in the case of index mismatching. For an anisotropic scattering, Eq. (2) should be changed as[23]

$$\Gamma'(r) = \exp(-\mu_t r_{i-1})[1 - R(n,\theta_i)] p(\cos \theta_i) \times$$
$$\mu_s \, \exp(-\mu_t r_i), \quad (5)$$

where $n = n_{i-1}/n_i$ is the refractive index ratio of the medium corresponding to photon path $\boldsymbol{r}_{i-1}$ and $\boldsymbol{r}_i$, and $R(n,\theta_i)$ is the Fresnel expression for specular reflection of the unpolarized light. Here, we only focus on the anisotropic scattering within the homogeneous medium, i. e., the reflection at the boundaries between media is ignored.
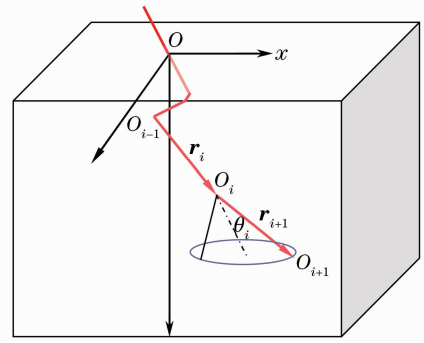

Fig. 1 A single photon incident on the slab at O and scattered in the fixed Cartesian coordinate system O-xyz. It experiences the ith scattering event at point O_i from O_{i-1} to O_{i+1}

2.2 Coordinate tracing method

To obtain the required probabilities that photons arrive to the detector, we need to integrate all the paths described by propagator length and vertex angle. As done in Ref. [25], the geometrical relationship of the path parameters is simple only for the single-vertex process. However, it becomes complicated for higher-order processes where not only the scattering angle θ but also the azimuthal angle φ are needed for geometrical expression. In fact, only single-vertex and double-vertex processes were expressed in Wang's work.

In order to model multiple-vertex processes, we introduce the coordinate tracing method. A fixed Cartesian coordinate system is chosen to trace photon movement, where the origin is set as the photon incident point on the tissue surface, the z-axis directs normally towards the interior of the medium, and the xy-plane is then parallel to the medium surface. Therefore, the photon history, $\boldsymbol{r} = \boldsymbol{r}_0 + \boldsymbol{r}_1 + \boldsymbol{r}_2 \cdots + \boldsymbol{r}_N$, can be described by the three orthogonal coordinates of the scattering points. If the coordinates of the scattering points, for example, $O_{i-1}(x_{i-1}, y_{i-1}, z_{i-1})$, $O_i(x_i, y_i, z_i)$, and $O_{i+1}(x_{i+1}, y_{i+1}, z_{i+1})$ are known, path lengths between $O_{i-1}(x_{i-1}, y_{i-1}, z_{i-1})$ and $O_i(x_i, y_i, z_i)$ or between $O_i(x_i, y_i, z_i)$ and $O_{i+1}(x_{i+1}, y_{i+1}, z_{i+1})$ can thus be obtained respectively as

$$r_{i-1} = \sqrt{(x_{i-1} - x_{i-2})^2 + (y_{i-1} - y_{i-2})^2 + (z_{i-1} - z_{i-2})^2}, \quad (6)$$

$$r_i = \sqrt{(x_i - x_{i-1})^2 + (y_i - y_{i-1})^2 + (z_i - z_{i-1})^2}, \quad (7)$$

and the scattering angle is given by

$$\theta_i = \cos^{-1}\left[\frac{(x_{i-1} - x_{i-2})(x_i - x_{i-1}) + (y_{i-1} - y_{i-2})(y_i - y_{i-1}) + (z_{i-1} - z_{i-2})(z_i - z_{i-1})}{r_{i-1} r_i}\right]. \quad (8)$$

In principle, the photon can be scattered to any direction after each scattering event. Therefore, the required probabilities that photons arrive at the detector can be simply expressed by the integral over all of the coordinates.

2.3 Probability distributions

In this section, we consider scattered photons passing through highly scattering homogeneous slab of thickness d with a definite incident angle θ_0 at the upper surface and finally arriving at the detector. Without loss of generality, here we chose the coordinates to let the incident light in the O-xz plane. The photon enters the slab at point $O(0,0,0)$ with an angle θ_0 to the direction of z, and $\theta_0 = 0$ is corresponding to the normal incidence.

2.3.1 Single-vertex processes

For single-vertex process, the photon is scattered only once. The scattered point, which is in the O-xz plane, is noted as $O_1(x_0, 0, z_0)$. The photon is scattered in the direction $\hat{r}_1$ and exits at point (x_1, y_1, d). In the case of index matching, the transmission probability density Γ_1 [per unit depth z_0 and per unit solid angle corresponding to the point (x_1, y_1, d)] of the set of single-interaction histories, can be written as

$$\Gamma_1 = \exp(-\mu_t r_0)\, p(\cos\theta_1)\mu_s \exp(-\mu_t r_1), \quad (9)$$

where

$$r_0 = z_0/\cos\theta_0, \quad x_0 = z_0\tan\theta_0,$$

$$r_1 = \sqrt{(x_1 - z_0\tan\theta_0)^2 + y_1^2 + (d - z_0)^2},$$

$$\theta_1 = \cos^{-1}\left[\frac{\sin\theta_0(x_1 - z_0\tan\theta_0) + \cos\theta_0(d - z_0)}{r_1}\right].$$

The solid angle element corresponding to the area element $\mathrm{d}S = \mathrm{d}x_1 \mathrm{d}y_1$ is $\mathrm{d}\Omega = \mathrm{d}x_1 \mathrm{d}y_1/r_1^2$. Therefore, the probability per unit area corresponding to the exiting point (x_1, y_1, d) of the single-interaction event can be obtained by integrating over depth z_0 for the corresponding probability density $\Gamma_1 r_1^2$ as

$$P_{S1}(x_1, y_1, d) = \int_0^d \mathrm{d}z_0\, \Gamma_1/r_1^2, \quad (10)$$

which describes the transmission-photon distribution at the outgoing surface.

It is required to integrate over both z_0 and the area in order to calculate the total transmission probability P_1 of all such single-vertex (i.e., single-interaction) paths within the medium. The integration limits are z_0 from 0 to d and x_1, y_1 from $-\infty$ to ∞. Then we have

$$P_1(d) = \int_0^d \mathrm{d}z_0 \int_{-\infty}^{+\infty} \mathrm{d}x_1 \int_{-\infty}^{+\infty} \mathrm{d}y_1\, \Gamma_1/r_1^2. \quad (11)$$

2.3.2 Double-vertex processes

For the photon interacting twice before emerging at the outgoing surface in transmission, the vertex and propagator terms may be written as

$$\Gamma_2 = \exp(-\mu_t r_0)\, p(\cos\theta_1)\mu_s \exp(-\mu_t r_1)\, p(\cos\theta_2)\mu_s \exp(-\mu_t r_2), \quad (12)$$

where

$$r_0 = z_0/\cos\theta_0, \quad x_0 = z_0\tan\theta_0,$$

$$r_1 = \sqrt{(x_1 - z_0\tan\theta_0)^2 + y_1^2 + (z_1 - z_0)^2},$$

$$\theta_1 = \cos^{-1}\left[\frac{\sin\theta_0(x_1 - z_0\tan\theta_0) + \cos\theta_0(z_1 - z_0)}{r_1}\right],$$

$$r_2 = \sqrt{(x_2 - x_1)^2 + (y_2 - y_1)^2 + (d - z_1)^2},$$

$$\theta_2 = \cos^{-1}\left[\frac{(x_1 - z_0\tan\theta_0)(x_2 - x_1) + y_1(y_2 - y_1) + (z_1 - z_0)(d - z_1)}{r_1 r_2}\right].$$

Correspondingly, the transmission-photon distribution at the outgoing surface is described by the probability per unit area at the emergence point (x_2, y_2, d) as

$$P_{S2}(x_2, y_2, d) = \int_0^d \mathrm{d}z_0 \int_0^d \mathrm{d}z_1 \int_{-\infty}^{+\infty} \mathrm{d}x_1 \int_{-\infty}^{+\infty} \mathrm{d}y_1\, \Gamma_2/(r_1 r_2)^2, \quad (13)$$

and the total transmission photon probability is obtained by integrating over the whole outgoing surface as

$$P_2(d) = \int_0^d \mathrm{d}z_0 \int_0^d \mathrm{d}z_1 \int_{-\infty}^{+\infty} \mathrm{d}x_1 \int_{-\infty}^{+\infty} \mathrm{d}y_1 \int_{-\infty}^{+\infty} \mathrm{d}x_2 \int_{-\infty}^{+\infty} \mathrm{d}y_2\, \Gamma_2/(r_1 r_2)^2. \quad (14)$$

2.3.3　High-order processes

　　The above mentioned method can be easily extended to high order vertex processes. Generally，for the photon N-times interacting before emerging at the outgoing surface in transmission，the vertex and propagator terms may be written as

$$\Gamma(r) = \exp(-\mu_t r_0)\,p(\cos\theta_1)\mu_s\exp(-\mu_t r_1)\,p(\cos\theta_2)\mu_s\exp(-\mu_t r_2)\cdots$$
$$\exp(-\mu_t r_{N-1})\,p(\cos\theta_N)\mu_s\exp(-\mu_t r_N)\,, \tag{15}$$

where，

$$r_0 = z_0/\cos\theta_0\,, \quad x_0 = z_0\tan\theta_0\,,$$

$$r_1 = \sqrt{(x_1 - z_0\tan\theta_0)^2 + y_1^2 + (z_1 - z_0)^2}\,,$$

$$\theta_1 = \cos^{-1}\left[\frac{\sin\theta_0(x_1 - z_0\tan\theta_0) + \cos\theta_0(z_1 - z_0)}{r_1}\right],$$

$$r_2 = \sqrt{(x_2 - x_1)^2 + (y_2 - y_1)^2 + (z_2 - z_1)^2}\,,$$

$$\theta_2 = \cos^{-1}\left[\frac{(x_1 - z_0\tan\theta_0)(x_2 - x_1) + y_1(y_2 - y_1) + (z_1 - z_0)(z_2 - z_1)}{r_1 r_2}\right],$$

$$\cdots$$

$$r_{N-1} = \sqrt{(x_{N-1} - x_{N-2})^2 + (y_{N-1} - y_{N-2})^2 + (z_{N-1} - z_{N-2})^2}\,,$$

$$r_N = \sqrt{(x_N - x_{N-1})^2 + (y_N - y_{N-1})^2 + (d - z_{N-1})^2}\,,$$

$$\theta_N = \cos^{-1}\left[\frac{(x_{N-1} - x_{N-2})(x_N - x_{N-1}) + (y_{N-1} - y_{N-2})(y_N - y_{N-1}) + (z_{N-1} - z_{N-2})(d - z_{N-1})}{r_{N-1} r_N}\right].$$

Correspondingly，the transmission-photon distribution at the outgoing surface is described by the probability per unit area at the point (x_N, y_N, d) as

$$P_{SN}(x_N, y_N, d) = \int_0^d \mathrm{d}z_0 \int_0^d \mathrm{d}z_1 \cdots \int_0^d \mathrm{d}z_{N-1} \int_{-\infty}^{+\infty}\mathrm{d}x_1 \int_{-\infty}^{+\infty}\mathrm{d}y_1 \int_{-\infty}^{+\infty}\mathrm{d}x_2 \int_{-\infty}^{+\infty}\mathrm{d}y_2 \cdots \int_{-\infty}^{+\infty}\mathrm{d}x_{N-1} \int_{-\infty}^{+\infty}\mathrm{d}y_{N-1} \Gamma_N/(r_1 r_2 \cdots r_{N-1} r_N)^2\,, \tag{16}$$

and the total transmission photon probability is obtained by integrating over the whole outgoing surface：

$$P_N(d) = \int_0^d \mathrm{d}z_0 \int_0^d \mathrm{d}z_1 \cdots \int_0^d \mathrm{d}z_{N-1} \int_{-\infty}^{+\infty}\mathrm{d}x_1 \int_{-\infty}^{+\infty}\mathrm{d}y_1 \int_{-\infty}^{+\infty}\mathrm{d}x_2 \int_{-\infty}^{+\infty}\mathrm{d}y_2 \cdots \int_{-\infty}^{+\infty}\mathrm{d}x_{N-1} \int_{-\infty}^{+\infty}\mathrm{d}y_{N-1} \int_{-\infty}^{+\infty}\mathrm{d}x_N \int_{-\infty}^{+\infty}\mathrm{d}y_N \Gamma_N/(r_1 r_2 \cdots r_{N-1} r_N)^2.$$
$$\tag{17}$$

3　Results and discussion

　　The scattering probabilities and probability-distributions are expressed as integrals over the corresponding coordinates. There are a lot of techniques to obtain the numerical integral results. For examples，the finite difference method is simple enough to conduct some simple integral calculations and the Monte Carlo method is generally used to calculate multiple integrals.

　　In this section，numerical results are presented for the slab medium with the assumed scattering coefficient $\mu_s = 2.1\ \mathrm{mm}^{-1}$，the extinction coefficient $\mu_t = 2.3\ \mathrm{mm}^{-1}$，the anisotropy parameter g varying between 0.15 and 0.9，and the assumed slab thickness ranging from 0 to 2.5 mm.

　　Figures 2，3，and 4 show the probabilities of photons traversing the scattering medium as a function of slab thickness for photons experiencing single-，double-，and four-scattering events described by Eqs. 11，14 and 17，respectively. The corresponding results are in good agreement with those
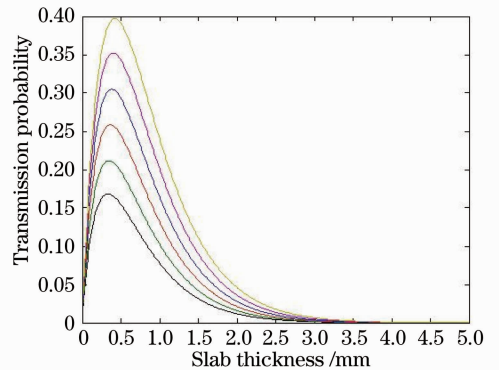
Fig. 2　Probability P_1 of a photon traversing a medium and undergoing single-scattering event as a function of slab thickness with $\mu_s = 2.1\ \mathrm{mm}^{-1}$ and $\mu_t = 2.3\ \mathrm{mm}^{-1}$ for increasing g from 0.15 to 0.9 in steps of 0.15 （form bottom to top）

based on the geometrical expressions[25] for single- and double-scattering events and the Monte Carlo stimulations[25] for four-scattering events. As shown in the Figs. 2，3，and 4，the probability profile of least-scattered photon is dependent on the in-

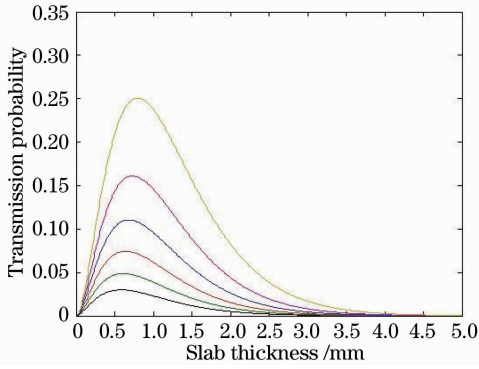Fig. 3 Probability P_2 of a photon traversing a medium and undergoing twice-scattering events as a function of slab thickness with $\mu_s = 2.1$ mm^{-1} and $\mu_t = 2.3$ mm^{-1} for increasing g from 0.15 to 0.9 in steps of 0.15 (form bottom to top)
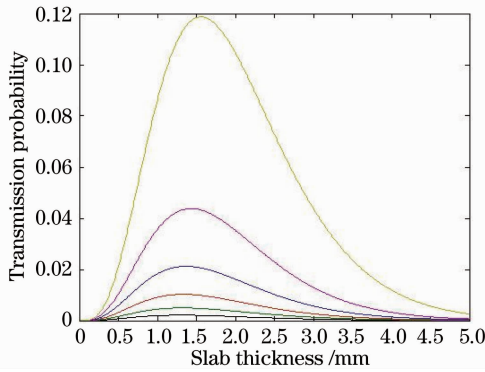

Fig. 4 Probability P_N ($N = 4$) of a photon traversing a medium and undergoing N time scattering events as a function of slab thickness with $\mu_s = 2.1$ mm^{-1}, $\mu_t = 2.3$ mm^{-1}, and $g = 0.9$
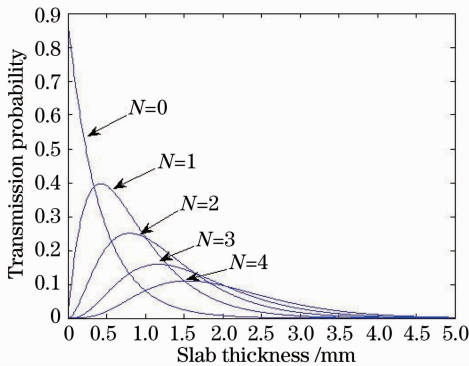
Fig. 5 Probabilities that a photon traversing a medium will undergo exactly N (up to 4) interactions as a function of thickness from the model prediction. Curves are shown for $\mu_s = 2.1$ mm^{-1}, $\mu_t = 2.3$ mm^{-1}, and $g = 0.9$

teraction times N and anisotropy parameter g, and it goes down as N increases and/or g decreases. For a specific N, the probability is maximized at about $d = N/\mu_t$, and the maximum probability moves to a smaller d slightly and decreases when g de-

creases. For a given value $g = 0.9$, the transmission probability profiles of the photons that have experienced exactly N (up to 4) interactions for the model predictions are plotted in Fig. 5.

In order to identify the relationships among the maximum probability P_{max} and N, g, P_{max} as a function of g are shown in Fig. 6 for $N = 1, 2, 3, 4$, respectively. For a certain N, ln P_{max} nearly linearly increases as g increases, and the more the interaction times N is, the larger the line slope is.
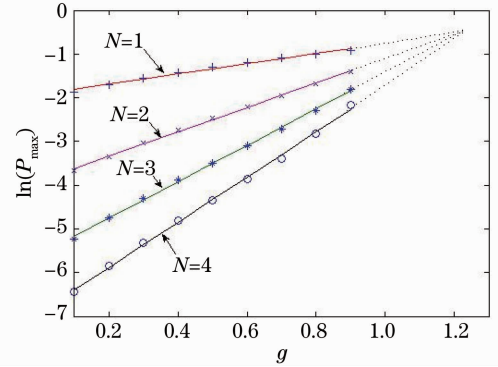

Fig. 6 Maximum probability P_{max} as a function of g for $N = 1, 2, 3$, and 4

For realistic applications, the detected photons are only those entering the detector window. Therefore we need to know the probability distribution at the output surface of the scattering medium. In case of medium thickness $d = 2$ mm and when normally incident light, i. e., incidence angle $\theta_0 = 0°$, is concerned, the traversing photon probability distributions at the output surface for single-scattering and double-scattered events are obtained from Eq. (9) and illustrated in Figs. 7 and 8 respectively. In can be seen that for normal incident light, the traversing photon has a symmetrical Gauss-like distribution around the incident light direction, and the distribution for double-scattered events (Fig. 8) is more dispersive than that for sin-
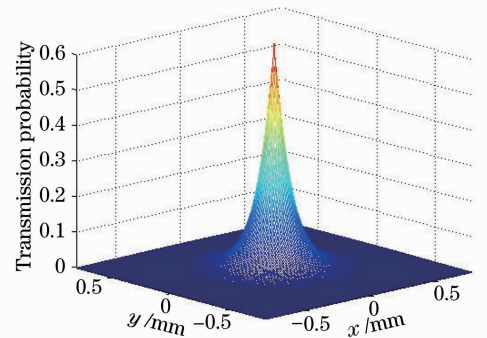

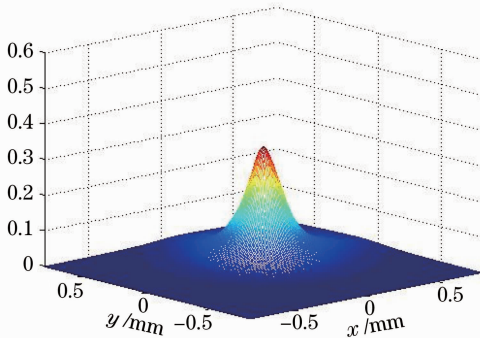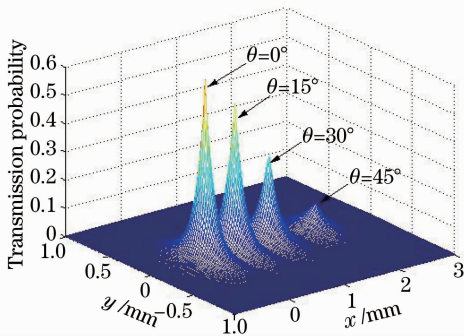Fig. 7 Probability distribution P_{S1} of a photon traversing a medium and undergoing single-scattering event for incident angle $\theta = 0°$ with $\mu_s = 2.1$ mm^{-1}, $\mu_t = 2.3$ mm^{-1}, $d = 2.0$ mm, and $g = 0.9$

gle-scattered events（Fig. 7）. The result implies that the dispersion is proportional to the interaction times that photon experiences. To consider the influence of incident angle on the probability distribution, Fig. 9 shows the probability distribution at $\theta_0 = 0°$, $15°$, $30°$, and $45°$ for single-scattered events. As shown in Fig. 9, the distribution becomes asymmetry and dispersed for oblique incident light. As the incident angle increases, the transmission probability decreases quickly. It will become very weak for incident angle greater than $45°$. The result indicates, for tissue optical measurement, that the incident light should be normal to the medium surface and the detector should be placed directly against the incident light to collect maximum scattered signals.

Fig. 8 Probability distribution P_{S2} of a photon traversing a medium and undergoing twice-scattering event for incident angle $\theta = 0°$ with $\mu_s = 2.1$ mm^{-1}, $\mu_t = 2.3$ mm^{-1}, $d = 2.0$ mm and $g = 0.9$

Fig. 9 Probability distribution P_{S1} of a photon traversing a medium and undergoing single-scattering event for incident angle $\theta = 0°, 15°, 30°$, and $45°$ with $\mu_s = 2.1$ mm^{-1}, $\mu_t = 2.3$ mm^{-1}, $d = 2.0$ mm, and $g = 0.9$

In conclusion, based on the vertex-propagator, the integral expressions of scattered photon probabilities for least-scattered photons traversing in a scattering medium have been obtained for photons experiencing any times interactions by the coordinate tracing method, and numerical results have been shown for transmission probability and distri-

bution as a function of scattered times, anisotropy parameter g, medium thickness, and incident angle. Compared with the methods based on both geometrical tracing and Monte Carlo simulation, our model is simpler and easier for programmming.

References

1 M. Rajadhyaksha, M. Grossman, D. Esterwitz *et al*.. In-vivo confocal scanning laser microscopy of human skin: melanin provides strong contrast[J]. *J. Invest. Dermatol*, 1995, **104**: 946~952

2 D. Huang, E. A. Swanson, C. P. Lin *et al*.. Optical coherence tomography[J]. *Science*, 1991, **254**: 1178~1181

3 Xing Da, Xiang Liangzhong. Photoacoustic imaging technique of tissue and its applications in biomedicine [J]. *Laser & Optoelectronics Progress*, 2007, **44**(8): 26~33
邢　达，向良忠. 生物组织的光声成像技术及其在生物医学中的应用[J]. 激光与光电子学进展，2007，**44**(8)：26~33

4 J. Mourant, I. Bigio, J. Boyer *et al*.. Spectroscopic diagnosis of bladder cancer with elastic light scattering[J]. *Lasers Surg. Med.*, 1995, **17**: 350~357

5 J. Fishkin, O. Coquoz, E. Anderson *et al*.. Frequency-domain photon migration measurements of normal and malignant tissue optical properties in a human subject[J]. *Appl. Opt.*, 1997, **36**: 10~20

6 Xu Xiangqun, Wu Liu. Influence of permeation characteristics of hyperosmotic agents on optical clearing of gastric tissue studied with near-infrared spectroscopy[J]. *Chinese J. Lasers*, 2005, **32**(5): 717~722
徐向群，吴　柳. 近红外光谱研究光透明齐渗透特性对胃组织光学透明的影响[J]. 中国激光，2005，**32**(5)：717~722

7 Xu Xiangqun, Wu Liu. Dependence on tissue structure of optical clearing with optical coherence tomography and near infrared spectroscopy[J]. *Chinese J. Lasers*, 2006, **33**(6): 998~1002
徐向群，吴　柳. 不同结构生物组织光透明作用比较[J]. 中国激光，2006，**33**(6)：998~1002

8 Xu X, Zhu Q. Sonophoretic delivery for contrast and depth improvement in skin optical coherence tomography[J]. *IEEE J. Sel. Top. Quantum Electron.*, 2008, **14**(1): 56~61

9 Xu X, Yu L, Chen Z. Optical clearing of flowing blood using dextrans with spectral domain optical coherence tomography[J]. *J. Biomed. Opt.*, 2008, **13**(2): 1~6

10 Xu X, Yu L, Chen Z. Effect of erythrocyte aggregation on hematocrit measurement using spectral domain optical coherence tomography[J]. *IEEE Trans. Biomed. Eng.*, 2008, **55**(12): 2753~2758

11 Wang L.-H., Jacques S. L., Zhang L.-Q.. MCML-Monte Carlo modelling of photon transport in multi-layered tissues [J]. *Computer Methods and Programs in Biomedicine*, 1995, **47**: 131~146

12 A. Ishimaru. Wave Propagation and Scattering in Random Media [M]. New York: Academic, 1978

13 K. Furutsu, Y. Yamada. Diffusion approximation for a dissipative random medium and the applications[J]. *Phys. Rew. E*, 1994, **50**: 1531~1560

14 M. Patterson, B. Chance, B. C. Wilson. Time resolved reflectance and transmittance for noninvasive measurement of tissue optical properties[J]. *Appl. Opt.*, 1989, **28**: 2331~2336

15 Zhu Dan, Wu Guiling, Luo Qingming *et al*.. Photonics diffusion for small source-detector separations of tissue[J]. *Acta Optica Sinica*, 2005, **25**(5): 638~642
朱　芍，吴龟灵 骆清铭 等. 生物组织中光子微区扩散理论研究[J]. 光学学报，2005，**25**(5)：638~642

16 R. Graaff, J. G. Aarnoudse, F. F. M. de Mul et al.. Light propagation parameters for anisotropically scattering media based on a rigorous solution of the transport equation[J]. Appl. Opt., 1989, 28: 2273~2279

17 P. Jenny, S. Mourad, T. Stamm et al.. Computing light statistics in heterogeneous media based on a mass weighted probability density function method[J]. J. Opt. Soc. Am. A, 2007, 24(8): 2206~2219

18 A. D. Kim. Transport theory for light propagation in biological tissue[J]. J. Opt. Soc. Am. A, 2004, 21(5): 820~827

19 R. F. Bonner, R. Nossal, S. Havlin et al.. Model for photon migration in turbid biological media[J]. J. Opt. Soc. Am. A, 1987, 4: 423~432

20 A. H. Gandjbakhche, R. Nossal, R. F. Bonner. Scaling relationships for theories of anisotropic random walks applied to tissue optics[J]. Appl. Opt., 1993, 32: 504~516

21 R. F. Lutomirski, A. P. Cievo, G. J. Hall. Moments of multiple scattering[J]. Appl. Opt., 1995, 34: 7125~7136

22 G. L. Rogers. Multiple path analysis of reflectance from turbid media[J]. J. Opt. Soc. Am. A, 2008, 25(11): 2879~2883

23 Y. Tsuchiya. Photon path distribution in inhomogeneous turbid media: theoretical analysis and a method of calculation[J]. J. Opt. Soc. Am. A, 2002, 19(7): 1383~1389

24 S. L. Jacques. Path integral description of light transport in tissue [J]. Ann. N. Y. Acad. Sci., 1998, 838: 1~13

25 R. K. Wang, M. Wilson. Vertex/propagator model for least-scattered photons traversing in a turbid medium[J]. J. Opt. Soc. Am. A, 2001, 18(1): 224~231

26 L. G. Henyey, J. L. Greenstein. Diffuse radiation in the galaxy [J]. Astrophys. J., 1941, 93: 70~83